Design of a Continuous Variable Transmission based Nuclear Decommissioning Robotic Arm

Rizuwana Parween, Kithmi N D Widanage, Hareesh Godaba, Nicolas Herzig, Yanan Li, Romeo Glovnea

***Abstract*— This work presents the design of a robotic manipulator for inspecting the cluttered environment inside a closed nuclear chamber with a narrow access port. We propose a Prismatic-Revolute-Revolute-Revolute (PRRR) joint based robotic manipulator and each joint is actuated by a continuous variable transmission (CVT) which can provide safe collision during inspection. We elaborate the design requirement, optimise the geometrical configuration of each link, and estimate the work-space of the manipulator. Analytically, we estimate the joint torque from static loading condition and based on the required torque, we optimise the geometrical configuration and material properties of the CVT, estimate the motor torque required for each joint and fix the transmission ratio of transmitting elements of each joint. Based on these data, the robot would be developed and safe collision performance of the CVT would be tested.**

I. INTRODUCTION

Decommissioning of a nuclear power station is a critical process in which its facilities are dismantled to the point where the risk by radiation is eliminated. This generally involves three stages as decontamination and dismantling, safe storage, and entombment [1]. Out of these, the decontamination and dismantling stage imposes a very specific set of challenges where many unknown variables affect the process. Especially, it is impossible to conduct operations such as inspection, monitoring, and size reduction and manipulation of contaminated materials such as debris and fuel, just by manual labour due to the high risk of contamination. Thus, robotic solutions are required to successfully tackle this challenge.

The development of robotic systems for nuclear decommissioning environments has been going on for several decades. From highly maneuverable multi-arm robotic platforms to disposable Vega ground robot, these have been used in different use-case scenarios in nuclear environments [2], [3], [4]. However, it should be noted that the challenges presented in different decommissioning tasks might vary.

One such use-case scenario is inspecting an enclosed cell chamber occupied by unknown obstacles. While the reachability and maneuverability should be inherently associated with a robotic manipulator deployed for such a task, another important aspect that should be considered is the collision-safe nature of the robotic manipulator itself. While navigation in unknown environments has been investigated in different robotic research works, many of them employ active impedance control methods which in fact are vulnerable to radiation due to the properties of the sensors employed. Therefore, in this work, we propose a design framework of a nuclear decommissioning robotic manipulator utilizing a novel, continuous variable transmission (CVT) based actuator providing safe collision in nuclear environments without sensor feedback.

Continuously variable transmissions have been used in applications including land vehicle transmission, machinery, mining equipment. Extensive research works have been done on validating the principles of operation of constant power (CP) toroidal type CVT for automotive applications [5], [6]. Here, we have attempted to extend the principle of CP-CVT for safe collision based robotic manipulator application. The

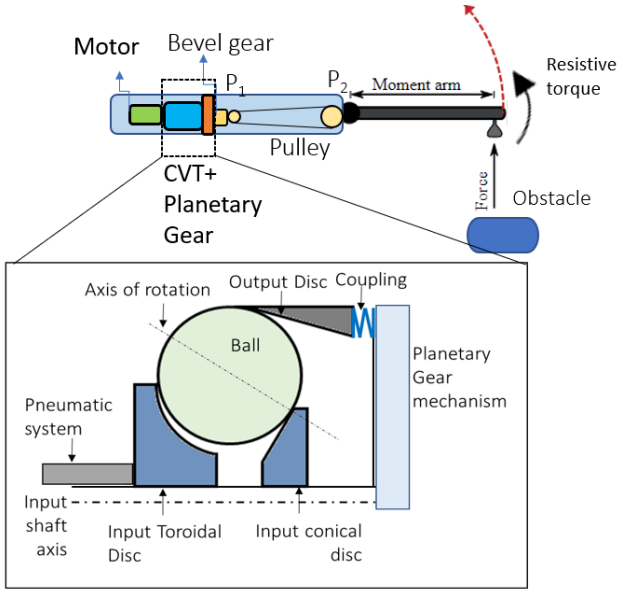

Fig. 1. Working principle of a CVT based robotic manipulator.

CVT has two discs fitted to the input shaft. One conical is fixed to the shaft and one toroidal which rotates with the shaft but also can translate along it [5], [6]. As illustrated in Fig.1, the power is transmitted from the input discs to a convenient number of intermediary spheres and from these to the output disc. The output disc transmits power to the output shaft via a coupling which plays the role of a torque-force converter. When the output torque increases the coupling forces the output disc to move axially, displacing the balls radially. This changes the angle of the axis of rotation of the balls and the distances between the points of contact between balls and

This work was funded by the United Kingdom Engineering and Physical Sciences Research Council (EPSRC) grant EP/W016168/1.

The authors are with the School of Engineering and Informatics, University of Sussex, United Kingdom, {R.Parween, k.dickwella-widanage, h.godaba, n.f.herzig, yl557, r.p.glovnea}@sussex.ac.uk

discs and their axes of rotation.

The paper is arranged as follows: Section II explains the design framework of the CVT based robotic manipulator, workspace generated by the manipulator, design details of the CVT, static torque required for the joints, estimation of the motor torque torque, and gear ratio required for the individual transmitting element of each link. Section III elaborates the discussion.

II. Design Framework for a CVT Based Robotic Manipulator

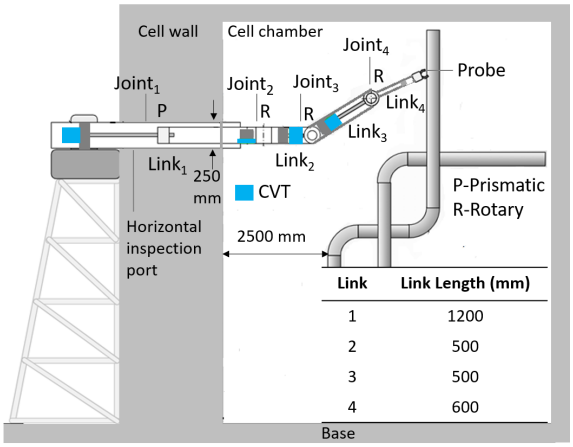

Fig. 2. Schematics showing cluttered environment inside an enclosed radiation environment.

The enclosed cell chamber consists of a main body with a thick wall and an inspection route, shown in Fig 2. The inspection route is approximately of 200-250 mm diameter. The enclosed cell chamber houses various obstacles (for example, network of cooling circuit pipes, frames, steel components and slabs, etc) which are approximately at a distance of 1-2.5 m from the inner surface of the inspection route. Hence, the length of the manipulator must be more than 1.5 m. The outer diameter of the manipulator must be within 0.02 m. The manipulator must have enough structural strength and redundant degrees of freedom to access the task-space. Considering these requirements, we design a robotic manipulator with circular cross-section that consists of four rigid links connected by joints (*PRRR*) as shown in Fig. 3(a). The end of the manipulator with prismatic joint is mounted inside the inspection port while the other end is free and used for performing inspection task with a probe. At the end-effector, we mount a probe of weight 0.012 kg for measuring the radiation level. Figures 3(b) and (c) show the geometrical configuration of the links. The lengths of Link_1, Link_2, Link_3, and Link_4 are given as 1.2 m, 0.5 m, 0.5 m, 0.6 m, respectively. The outer diameter and shell thickness of Link_1, Link_2, Link_3 are considered as 200 mm and 3 mm, respectively. The outer diameter and shell thickness of Link_4 are considered as 40 mm and 3 mm, respectively.

A. Workspace Analysis

Figures 3(a) and (b) show the link geometry and kinematic frame assignment at each joint, respectively. The Denavit–Hartenberg (D-H) parameters associated with each joint is shown in Fig. 3(c).

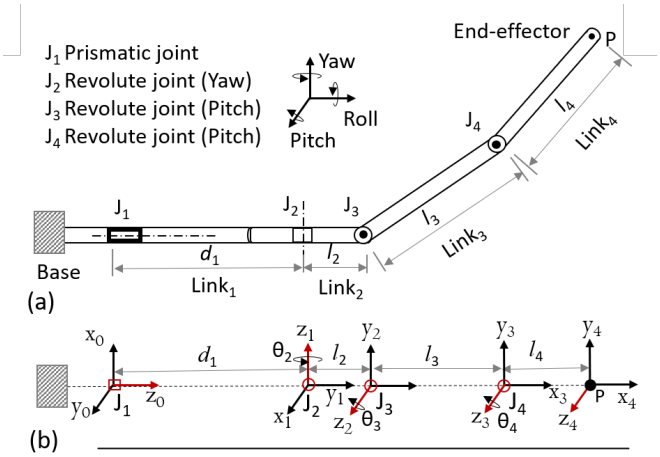

Joint	Joint Distance (mm)	Joint Angle (degree)	Link length (mm)	Twist Angle (degree)
1	d_1	90	0	90
2	0	θ_2	l_2	90
3	0	θ_3	l_3	0
4	0	θ_4	l_4	0

(c)

Fig. 3. (a) Schematics of the robot arm, (b) Assignment of the kinematic frames to each link, (c) D-H parameters associated with each joint.

The transformation matrix between each of the frame is given by Equations (1)-(4). The composite transformation matrix that transforms the joint 1 to the end effector is ${}^0T_4 = {}^0T_1\,{}^1T_2\,{}^2T_3\,{}^3T_4$.

$$ {}^0T_1 = \begin{bmatrix} 0 & 0 & 1 & 0 \\ 1 & 0 & 0 & 0 \\ 0 & 1 & 0 & d_1 \\ 0 & 0 & 0 & 1 \end{bmatrix} \tag{1} $$

$$ {}^1T_2 = \begin{bmatrix} \cos\theta_2 & 0 & \sin\theta_2 & l_2\cos\theta_2 \\ \sin\theta_2 & 0 & -\cos\theta_2 & l_2\sin\theta_2 \\ 0 & 1 & 0 & 0 \\ 0 & 0 & 0 & 1 \end{bmatrix} \tag{2} $$

$$ {}^2T_3 = \begin{bmatrix} \cos\theta_3 & -\sin\theta_3 & 0 & l_3\cos\theta_3 \\ \sin\theta_3 & \cos\theta_3 & 0 & l_3\sin\theta_3 \\ 0 & 0 & 1 & 0 \\ 0 & 0 & 0 & 1 \end{bmatrix} \tag{3} $$

$$ {}^3T_4 = \begin{bmatrix} \cos\theta_4 & -\sin\theta_4 & 0 & l_4\cos\theta_4 \\ \sin\theta_4 & \cos\theta_4 & 0 & l_4\sin\theta_4 \\ 0 & 0 & 1 & 0 \\ 0 & 0 & 0 & 1 \end{bmatrix} \tag{4} $$

$$
\begin{aligned}
P_x &= l_3 \sin\theta_3 + l_4 \sin(\theta_3+\theta_4) \\
P_y &= \cos\theta_2 [l_2 + l_3 \cos\theta_3 + l_4 \cos(\theta_3+\theta_4)] \\
P_z &= d_1 + \sin\theta_2 [l_2 + l_3 \cos\theta_3 + l_4 \cos(\theta_3+\theta_4)]
\end{aligned} \tag{5}
$$

Equation 5 shows the position of the end-effector, given by (P_x, P_y, P_z). The configuration of the manipulator including the length of each link, the allowed range of joint motions decides the workspace. Considering the mechanical constraint of the revolute joints, we have set the joint limits on $\theta_2, \theta_3, \theta_4$, in the range of -80 to 80 degrees. Figure 4 represents the reach of its end-effector and its three dimensional work envelope.

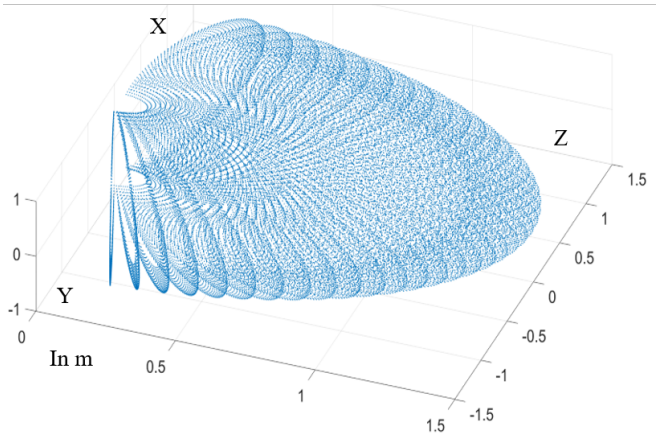

Fig. 4. Work-space of the robotic arm inside the cell chamber.

B. Estimation of Static Joint Torque

Each joint consists of a CVT actuator as shown in Fig. 1(d). The CVT for the joint J_2 is designed based on the frictional torque required at the bearing. Here, we consider that the movement of the robotic arm is in the range of 2-4 rpm. Hence, the CVTs for J_3 and J_4 are designed based on the torque estimated from the static loading. The CVT for the prismatic joint is based on the torque required for the lead screw to have an extension of 1.2 m. We assume the weight of the motor (w_m), CVT (w_c), additional components (w_a), end-effector (w_e) as 40 N, 40 N, 20 N, and 1.2 N respectively. From the static equilibrium analysis, we obtain the following expressions.

$$
\begin{aligned}
\tau_4 &= w_e l_4 + w_3 \frac{l_4}{2} \\
\tau_3 &= w_e(l_4+l_3) + w_4(l_3+\frac{l_4}{2}) + (w_3+w_m+w_c+w_a)\frac{l_3}{2} \\
R_2 &= w_4 + w_3 + w_2 + w_e + 2w_m + 2w_c + 3w_a
\end{aligned} \tag{6}
$$

Considering all the dimension and wight details, we obtain the torque at J_4 (τ_4), J_3 (τ_3) as 2.9 Nm and 38.9 Nm respectively. The vertical reaction force at J_2 (R_2) is 297 N. From ASME standard of the bearing design, the frictional toque is estimated as 1.4 Nm. The torque required for the lead screw mechanism for J_1 is around 0.95 Nm.

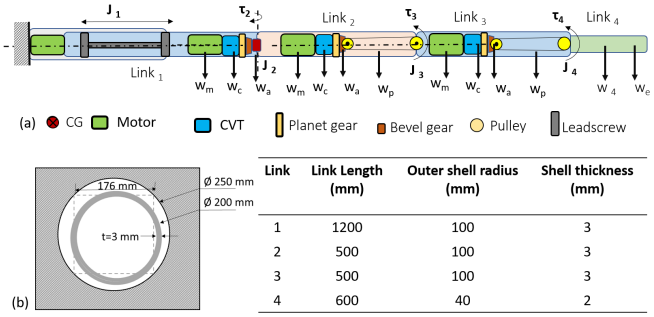

Link	Link Length (mm)	Outer shell radius (mm)	Shell thickness (mm)
1	1200	100	3
2	500	100	3
3	500	100	3
4	600	40	2

Fig. 5. (a) Static loading condition at home position of the manipulator, (b) Geometrical details of each link.

For CVT kinematic and dynamic analysis, we refer the paper by Glovnea et al. [5], [6]. Figure 6 shows the geometrical configuration of the CVT. The transmission ratio of a CVT depends on the geometrical configuration of the toroidal disc (major radius, minor radius), material properties and dimension of the ball, angle between the horizontal and the contact point of the toroidal disc, conical disc and output disc with the ball. The external forces applied by the pneumatic system on the toroidal disc (F_a) modulate the torque required to be transmitted.

While designing the CVT, the minor and major radii of the toroidal disc are constrained by the shaft diameter and the port dimension, respectively. The radius of the ball is constrained by the inertia and contact pressure generated at the contact boundary of the balls and disc. The ball speed has to be more than 40 mm/sec. The external force supplied by a pneumatic system regulates the torque transmission via CVT. The transmitted torque is also limited by the contact pressure which depends on the material properties of the ball.

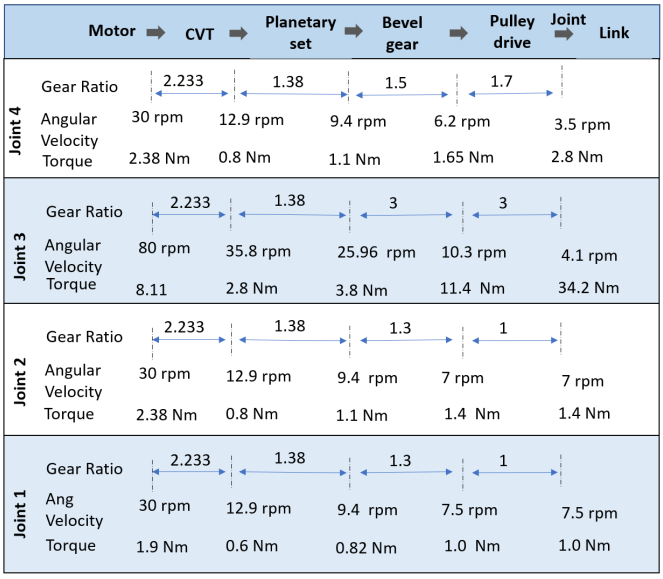

Fig. 6. Gear ratio for the transmitting elements for the joints.

Based on trial and error, we observe that for all com-

binations of the axial force in the range of 40 N- 170 N and input speed 30 rpm- 80 rpm, the contact pressures at the contact points of the ball with the toroidal, conical and output disc are found to be below 2 GPa. In addition, the contact velocities at these contact points are more than 30 mm/s. Hence, from tribology point of view, the design is safe. For an external force of 40 N and input CVT speed of 30 rpm, the output torque at the CVT is 0.6 Nm. For an external force of 50 N and input CVT speed of 30 rpm, the output torque at the CVT is 0.8 Nm. For an external force of 50 N and input CVT speed of 30 rpm, the output torque at the CVT is 2.8 Nm. We have estimated the motor torque required for J_1, J_2, J_3 and J_4 as 1.9 Nm, 2.38 Nm, 8.11 Nm and 2.38 Nm, respectively. This torque is the total torque required by the motor to operate the CVT.

III. Discussion and Summary of Work

In this study, we have presented the design of the robotic arm based on static loading conditions. It is due to the fact that the arm is assumed to be operated at a low speed (approximately 4-5 rpm) for inspection. However, the dynamics and inertial loading need to be considered for high-speed applications. Based on the design requirements, we have optimised the geometrical configuration of the robotic arm, estimated the work-space of the end-effector and finalised the range of motion of each joint. From static equilibrium, we have estimated the torque required for the revolute joints (J_3 and J_4) used for vertical movement. For horizontal motion of the joint J_2, we have estimated the motor torque requirement based on friction at the bearing. For the prismatic joint, we have selected the lead screw dimensions and estimated the required torque. Based on these estimated torques, we have designed the CVT and selected the joint components and finalised their transmission ratio. In future, we will fabricate CVT and select the other components of the robotic arm and experimentally validate the proposed design.

References

[1] Y. A. Suh, C. Hornibrook, and M.-S. Yim, "Decisions on nuclear decommissioning strategies: Historical review," *Progress in Nuclear Energy*, vol. 106, pp. 34–43, 2018. [Online]. Available: https://www.sciencedirect.com/science/article/pii/S0149197018300234

[2] M. J. Bakari, K. M. Zied, and D. W. Seward, "Development of a multi-arm mobile robot for nuclear decommissioning tasks," *International Journal of Advanced Robotic Systems*, vol. 4, no. 4, p. 51, 2007. [Online]. Available: https://doi.org/10.5772/5665

[3] C. J. Taylor and D. Robertson, "State-dependent control of a hydraulically actuated nuclear decommissioning robot," *Control Engineering Practice*, vol. 21, no. 12, pp. 1716–1725, 2013. [Online]. Available: https://www.sciencedirect.com/science/article/pii/S0967066113001573

[4] B. Bird, M. Nancekievill, A. West, J. Hayman, C. Ballard, W. Jones, S. Ross, T. Wild, T. Scott, and B. Lennox, "Vega—a small, low cost, ground robot for nuclear decommissioning," *Journal of Field Robotics*, vol. 39, no. 3, pp. 232–245, 2022. [Online]. Available: https://onlinelibrary.wiley.com/doi/abs/10.1002/rob.22048

[5] C. A. Bell, C. Mares, and R. P. Glovnea, "Concept design optimisation for continuously variable transmissions," *International Journal of Mechatronics and Manufacturing Systems*, vol. 4, no. 1, pp. 19–34, 2011.

[6] C. A. Bell and R. P. Glovnea, "Modelling and simulation of a novel, toroidal-type, cvt (traction drives)," in *The Proceedings of the JSME international conference on motion and power transmissions 2009*. The Japan Society of Mechanical Engineers, 2009, pp. 672–676.